Revista Facultad de Ingeniería

UNIVERSIDAD DE ANTIOQUIA

Title: **Chaotic intermittency with non-differentiable *M(x)* function**

Authors: Sergio Elaskar[1], https://orcid.org/0000-0002-7250-0392, Ezequiel del Río[2] https://orcid.org/0000-0003-3384-9521, Mauro Grioni* https://orcid.org/0000-0002-0269-9383

[1] Department of Aeronautical, National University of Córdoba, Argentina and National Scientific and Technical Research Council (CONICET). Argentina.
[2] Departamento de Física Aplicada, Universidad Politécnica de Madrid. Madrid, España.
[3] Institute of Structural Mechanics and Seismic Risk (IMERIS). National University of Cuyo. Argentina

Corresponding Author: Mauro Grioni
E-mail mauro.grioni@ingenieria.uncuyo.edu.ar

DOI: **10.17533/udea.redin.20230110**

To appear in: *Revista Facultad de Ingeniería Universidad de Antioquia*

Received: October 25, 2022
Accepted: January 27, 2023
Available Online: January 27, 2023

Please cite this article as: S. Elaskar, E. Del Rio and M. Grioni. Chaotic intermittency with non-differentiable *M(x)* function, *Revista Facultad de Ingeniería Universidad de Antioquia*. [Online]. Available: https://www.doi.org/10.17533/udea.redin.20230110 redin Revista Facultad de Ingeniería, January 26, 2023

Chaotic intermittency with non-differentiable $M(x)$ function

Intermitencia caótica con función $M(x)$ no diferenciable

Authors: Double-blind review

KEYWORDS:
intermittency, reinjection, discontinuous reinjection probability density function

intermitencia, reinyección, función de densidad de probabilidad de reinyección discontinua

ABSTRACT: One-dimensional maps showing chaotic intermittency with discontinuous reinjection probability density functions are studied. For these maps, the reinjection mechanism possesses two different processes. The M function methodology is applied to analyze the complete reinjection mechanism and to determine the discontinuous reinjection probability density function. In these maps, the function $M(x)$ is continuous and non-differentiable. Theoretical equations are found for the function $M(x)$ and for the reinjection probability density function. Finally, the theoretical results are compared with numerical data finding high accuracy.

RESUMEN: En este trabajo se estudian mapas unidimensionales que muestran intermitencia caótica con funciones de densidad de probabilidad de reinyección discontinuas. Para estos mapas, el mecanismo de reinyección posee dos procesos diferentes. Para analizar el mecanismo de reinyección completo y determinar la función de densidad de probabilidad de reinyección discontinua, se aplica la metodología de la función M. Dicha función es continua y no derivable. Se encuentran ecuaciones teóricas para la función $M(x)$ y para la función de densidad de probabilidad de reinyección. Finalmente, los resultados teóricos se comparan con datos numéricos encontrándose una alta precisión entre ambos.

1. Introduction

Non-linear behavior is a ubiquitous feature in natural phenomena and human-made mechanisms. Several of these non-linear behaviors are described by dynamical systems displaying chaos. A route by which the solutions of the non-linear dynamical systems can evolve from regular to chaotic behavior is chaotic intermittency [1]. The system solutions are composed of laminar and chaotic phases. The laminar or regular phases are pseudo-equilibrium or pseudo-periodic solutions, while the bursts correspond to chaotic evolution [1–3].

The phenomenon of chaotic intermittency has been found in different fields of science as physics, chemistry, medicine, engineering, and economics [4–16]. Therefore, a better description and understanding of the chaotic intermittency phenomenon would contribute to several fields of knowledge.

Chaotic intermittency was classified into three types named I, II, and III, following the loss of stability for maps [17]. Type I intermittency happens if there is a tangent bifurcation and an eigenvalue leaves the unit circle across +1. Type II intermittency occurs by a Hopf bifurcation, and two complex-conjugate eigenvalues move away from the unit circle. Finally, type III takes place during a subcritical period-doubling bifurcation, and an eigenvalue escapes the unit circle by -1 [1][3]. Posterior research detected other intermittency types, such as X, on-off, V, eyelet, and ring [18–27].

In one-dimensional maps, intermittency is produced by a specific local map and a reinjection mechanism [1][2]. The local map defines the type of intermittency, and the reinjection process returns the trajectories to the laminar zone. The reinjection probability density function (RPD function) determines the trajectories' probability of being reinjected in the laminar zone or interval [1–3].

The correct description of the RPD function is essential for understanding the intermittency phenomenon. Several approaches were utilized to calculate the RPD function, being the uniform reinjection (a constant RPD) the most implemented [2][3][17][28]. Recently, a more general methodology to evaluate the RPD function has been introduced [1], which is called the M function methodology. This methodology has accurately worked for types I, II, III, and V intermittencies with and without noise [29–35].

This paper extends the M function methodology to evaluate discontinuous RPD functions. These RPDs are related to two o more overlapping reinjection mechanisms [1][29][36]. The paper shows that discontinuous RPD functions correspond to non-differentiable $M(x)$ functions.

The paper is organized into five sections. The second section briefly describes the M function methodology. Section 3 extends the M function methodology to evaluate discontinuous RPD functions. In Section 4, numerical tests are presented. Finally, in Section 5 there are the main conclusions.

2. The $M(x)$ function

The RPD function determines the statistical distribution of trajectories leaving the chaotic region and going back into the laminar region. The RPD is the more significant function in describing chaotic intermittency behavior. Once the RPD function is known, the other statistical properties can be determined [1][2].

To evaluate the RPD function, here also called $\phi(x)$, we introduce the following function (see equation (1)) [1]:

$$M(x)=\begin{cases}\frac{\int_{\hat{x}}^{x} y\,\phi(y)\,dy}{\int_{\hat{x}}^{x}\phi(y)\,dy} & \text{if } \int_{\hat{x}}^{x}\phi(y)dy\neq 0\\ 0 & \text{otherwise}\end{cases} \quad (1)$$

$\hat{x}$ is the lower boundary of reinjection, and $\hat{x}\leq x\leq x_0+c$. Where x_0 is the vanished or unstable fixed point and the laminar interval is $L=[\hat{x},x_0+c]$. In addition, $\phi(x)$ is a C^1 function in L, where a C^q is a q times continuously differentiable function.

The $M(x)$ function has been extensively used to determine the statistical properties in chaotic intermittency (see [1][29–35] and references indicated in these manuscripts).

In several maps showing intermittency, the $M(x)$ function showed in equation (2) is a linear function [1]

$$M(x)=\begin{cases} m(x-\hat{x})+\hat{x} & \text{if } \ x\geq\hat{x}\\ 0 & \text{otherwise}\end{cases} \quad (2)$$

where $m\in(0,1)$ is a free parameter. Note, the $M(x)$ function is defined in the laminar interval $[\hat{x},x_0+c]$.

Theorem. Let $M(x)$ be a function defined by equation (1) and $\phi(x)$ is a C^1 function. If $M(x)$ is the linear function given by equation (2). Then, the reinjection probability density function results in equation (3):

$$\phi(x)=b\,(x-\hat{x})^{\frac{1-2m}{m-1}} \quad (3)$$

Proof. For $\int_{\hat{x}}^{x}\phi(y)dy\neq 0$ the equation (1) can be written as expressed in equation (4),

$$M(x)\int_{\hat{x}}^{x}\phi(y)\,dy=\int_{\hat{x}}^{x} y\,\phi(y)\,dy \quad (4)$$

If we differentiate this equation twice with x, we get the equation (5),

$$\frac{d^2M(x)}{dx^2}\int_{\hat{x}}^{x}\phi(y)\,dy+2\left(\frac{dM(x)}{dx}-1\right)\phi(x)+ (M(x)-x)\frac{d\phi(x)}{dx}=0 \quad (5)$$

if we assume that $M(x)$ is given by equation (2), we obtain $\frac{d^2M(x)}{dx^2}=0$, and $\frac{dM(x)}{dx}=m$, hence the equation (5) results in equation (6),

$$\frac{d\phi(x)}{dx}\,(x-\hat{x})\,(m-1)+\phi(x)(2m-1)=0 \quad (6)$$

The RPD function (see equation (7)) is calculated by integration of the last equation

$$\phi(x)=b\,(x-\hat{x})^{\frac{1-2m}{m-1}} \quad (7)$$

where b is the integration constant.

Therefore, the RPD function can be written as expressed in equation (8),

$$\phi(x)=b(\alpha)\,(x-\hat{x})^{\alpha} \quad \text{where} \quad \alpha=\frac{1-2m}{m-1} \quad (8)$$

$b(\alpha)$ is a normalization parameter selected to verify $\int_L \phi(x)\,dx=1$, where L is the laminar interval.

To approximate numerically the $M(x)$ function, we notice that it is an average over reinjection points in the interval $[\hat{x},x]$, then we can write the equation (9) as follows

$$M(x)=M_j\equiv\frac{1}{j}\sum_{k=1}^{j}x_k,\qquad x_{j-1}<x\leq x_j \quad (9)$$

where the data set (N reinjection points) $\{x_j\}_{j=1}^{N}$ has been previously ordered, i.e., $x_j\leq x_{j+1}$. Therefore, $\hat{x}$ can be approximated by $\hat{x}\approx\inf\{x_j\}$.

We highlight the $M(x)$ function is a useful mathematical tool to calculate $\hat{x}$ and α determining the RPD function and other statistical properties in chaotic intermittency. Several papers have verified that $M(x)$ is a linear function, and the RPD function is given by equation (8) (see [1][29][31][32] and references indicated in these manuscripts).

3. Non-differentiable $M(x)$ function

In this section, we analyze the reinjection mechanisms that display non-differentiable functions $M(x)$. These cases happen when there are two o more reinjection processes generating discontinuous RPD functions. Accordingly, $\phi(x)$ is not C^1 as in the previous section.

Here we introduce a general methodology to describe the $M(x)$ function and to obtain the RPD function when there are two different reinjection processes.

Let us consider a generic one-dimensional map $x_{n+1} = F(x_n)$, which has two reinjection processes, called here a and b, respectively. Each reinjection process verifies a linear $M(x)$ function (see equation (2)). We call $M_a(x)$ and $M_b(x)$ these functions for each reinjection process, and they verify the equation (10),

$$\begin{aligned} M_a(x) &= m_a(x - \hat{x}_a) + \hat{x}_a \\ M_b(x) &= m_b(x - \hat{x}_b) + \hat{x}_b \end{aligned} \tag{10}$$

where $\hat{x}_a$ and $\hat{x}_b$ are the lower boundary of reinjection for the reinjection processes a and b respectively.

From equation (10) and using the theory described in Section 2, we get two independent RPD functions as expressed in equation (11),

$$\begin{aligned} \phi_a(x) &= b_a(\alpha_a)\,(x - \hat{x}_a)^{\alpha_a}, \quad \alpha_a = \tfrac{1-2m_a}{m_a-1} \\ \phi_b(x) &= b_b(\alpha_b)\,(x - \hat{x}_b)^{\alpha_b}, \quad \alpha_b = \tfrac{1-2m_b}{m_b-1} \end{aligned} \tag{11}$$

We analyze two general cases. The first one assumes that the overlap of the reinjection processes occurs in the lower part of the laminar interval. On the other hand, the second case considers that the reinjection processes superposition happens in the upper part of the laminar interval.

3.1 Case 1. Reinjection overlapping in the lower part of the laminar interval

First, we study the case with reinjection overlap or superposition in the lower part of the laminar interval. Then, the complete RPD function results in equation (12),

$$\phi(x) = \begin{cases} \phi_1(x) = \phi_a(x) + \phi_b(x), & \hat{x}_b \le x \le x_s \\ \phi_2(x) = \phi_b(x), & x_s < x \le x_0 + c \end{cases} \tag{12}$$

where x_s is the non-differentiable point for the global $M(x)$ function.

Since $b_a(\alpha_a)$ and $b_b(\alpha_b)$ are real numbers, we can write $b_a(\alpha_a) = b$, and $b_b(\alpha_b) = k\,b$. Where k is a real number, and b is evaluated from the normalization condition, which is (see [1, 2])

$$\int_{\hat{x}_b}^{x_0+c} \phi(x)\,dx = 1 \tag{13}$$

If we introduce equations (11) and (12) in equation (13), we get equation (14)

$$k\,b \int_{\hat{x}_b}^{x_0+c} (x - \hat{x}_b)^{\alpha_b} dx + b \int_{\hat{x}_a}^{x_s} (x - \hat{x}_a)^{\alpha_a} dx = 1 \tag{14}$$

where $x_0 + c$ is the upper limit of the laminar interval, $L = [\hat{x}_b, x_0 + c]$, and we have assumed $\hat{x}_b = \hat{x}_a$ (see equation (12)). We emphasize, without loss of generality, that $\hat{x}_b$ could coincide with $x_0 - c$. Note that k and b, are always real numbers because (see equation (14))

$$\begin{aligned} (x - \hat{x}_b)^{\alpha_b} \ge 0 \quad &\text{if} \quad \hat{x}_b \le x \le x_0 + c \\ (x - \hat{x}_a)^{\alpha_a} \ge 0 \quad &\text{if} \quad \hat{x}_a \le x \le x_s \end{aligned} \tag{15}$$

In equation (12), we have considered that $\phi_1(x)$ is determined by two reinjection mechanisms represented by $\phi_a(x)$ and $\phi_b(x)$, while $\phi_2(x)$ is calculated by only one reinjection mechanism given by $\phi_b(x)$.

Note $\phi_b(x)$ is defined in the complete laminar interval L. However, $\phi_a(x)$ acts only in the sub-interval $[\hat{x}_b, x_s]$. To calculate the global $M(x)$ function, we implement the M function methodology introduced in the previous section.

Therefore, the complete $M(x)$ function is given by equations (16) and (17).

We notice the complete $M(x)$ function has a non-differentiable point at $x = x_s$. Also, note the $M(x)$ function does not depend on the normalization factor b. However, it depends on k. The parameter k is calculated from equation (17), and it is given by equation (18). In this equation, $M(x)$ and x are considered for all reinjected points verifying $x > x_s$, and k is calculated as the average of them.

3.2 Case 2. Reinjection overlapping in the upper part of the laminar interval

Now, we study the second case, where the reinjection processes overlapping happens in the upper part of the laminar interval. Therefore, the RPD function can be written as expressed in equation (19):

$$\phi(x) = \begin{cases} \phi_1(x) = \phi_a(x), & x_0 - c \le x < x_s \\ \phi_2(x) = \phi_a(x) + \phi_b(x), & x_s \le x \le x_0 + c \end{cases} \tag{19}$$

where $\phi_a(x)$ and $\phi_b(x)$ are obtained as shown in equation (20):

$$\begin{aligned} \phi_a(x) &= b\,(x - \hat{x}_a)^{\alpha_a} = b\,(x - x_0 + c)^{\alpha_a} \\ \phi_b(x) &= b\,k\,(x - \hat{x}_b)^{\alpha_b} = b\,k\,(x - x_s)^{\alpha_b} \end{aligned} \tag{20}$$

where x_0 is the fixed point of the map, and the laminar interval is $L = [x_0 - c, x_0 + c]$. Note that $\hat{x}_a = x_0 - c$ is the lower limit of the laminar interval, L, and $\hat{x}_b = x_s$. Then, the M functions are obtained in equation (21) as follows

$$\begin{aligned} M_a(x) &= m_a\,(x - x_0 + c) + x_0 - c \\ M_b(x) &= m_b(x - x_s) + x_s \end{aligned} \tag{21}$$

For $x \le x_s$, the function $M(x)$ is

$$\begin{aligned} M(x) &= \frac{\int_{\hat{x}_a}^{x} y\,\phi_a(y)\,dy+\int_{\hat{x}_b}^{x} y\,\phi_b(y)\,dy}{\int_{\hat{x}_a}^{x} \phi_a(y)\,dy+\int_{\hat{x}_b}^{x} \phi_b(y)\,dy} = \frac{\int_{\hat{x}_a}^{x} y\,b\,(y-\hat{x}_a)^{\alpha_a}\,dy+\int_{\hat{x}_b}^{x} y\,b\,k\,(y-\hat{x}_b)^{\alpha_b}\,dy}{\int_{\hat{x}_a}^{x} b\,(y-\hat{x}_a)^{\alpha_a}\,dy+\int_{\hat{x}_b}^{x} b\,k\,(y-\hat{x}_b)^{\alpha_b}\,dy} \\ &= \frac{(-\hat{x}_a+x)^{1+\alpha_a}(\hat{x}_a+x(1+\alpha_a))\,(1+\alpha_b)(2+\alpha_b)+k(x-\hat{x}_b)^{1+\alpha_b}(\hat{x}_b+x(1+\alpha_b))\,(1+\alpha_a)(2+\alpha_a)}{(2+\alpha_a)(2+\alpha_b)\,((-\hat{x}_a+x)^{1+\alpha_a}\,(1+\alpha_b)+k(x-\hat{x}_b)^{1+\alpha_b}\,(1+\alpha_a))} \end{aligned} \tag{16}$$

And, for $x > x_s$

$$\begin{aligned} M(x) &= \frac{\int_{\hat{x}_a}^{x_s} y\,\phi_a(y)\,dy+\int_{\hat{x}_b}^{x} y\,\phi_b(y)\,dy}{\int_{\hat{x}_a}^{x_s} \phi_a(y)\,dy+\int_{\hat{x}_b}^{x} \phi_b(y)\,dy} = \frac{\int_{\hat{x}_a}^{x_s} y\,b\,(y-\hat{x}_a)^{\alpha_a}\,dy+\int_{\hat{x}_b}^{x} y\,b\,k\,(y-\hat{x}_b)^{\alpha_b}\,dy}{\int_{\hat{x}_a}^{x_s} b\,(y-\hat{x}_a)^{\alpha_a}\,dy+\int_{\hat{x}_b}^{x} b\,k\,(y-\hat{x}_b)^{\alpha_b}\,dy} \\ &= \frac{(x_s-\hat{x}_a)^{1+\alpha_a}(\hat{x}_a+x_s(1+\alpha_a))\,(1+\alpha_b)(2+\alpha_b)+k(x-\hat{x}_b)^{1+\alpha_b}(\hat{x}_b+x(1+\alpha_b))\,(1+\alpha_a)(2+\alpha_a)}{(2+\alpha_a)(2+\alpha_b)\,((x_s-\hat{x}_a)^{1+\alpha_a}\,(1+\alpha_b)+k(x-\hat{x}_b)^{1+\alpha_b}\,(1+\alpha_a))} \end{aligned} \tag{17}$$

$$k = \frac{M(x)\,(2+\alpha_a)(2+\alpha_b)\,((x_s-\hat{x}_a)^{1+\alpha_a}\,(1+\alpha_b)-(x_s-\hat{x}_a)^{1+\alpha_a}(\hat{x}_a+x_s(1+\alpha_a))\,(1+\alpha_b)(2+\alpha_b)}{(x-\hat{x}_b)^{1+\alpha_b}(\hat{x}_b+x(1+\alpha_b))\,(1+\alpha_a)(2+\alpha_a)-M(x)\,(2+\alpha_a)(2+\alpha_b)(1+\alpha_a)(x-\hat{x}_b)^{1+\alpha_b}} \tag{18}$$

$M_a(x)$ is defined inside the complete laminar interval $L = [x_0-c, x_0+c]$. However, $M_b(x)$ is given in $[x_s, x_0+c]$.
We calculate the parameters m_a and m_b, for each reinjection process individually. We apply the M function methodology previously explained. Then, α_a and α_b are obtained in equation (22) as follows

$$\alpha_a = \frac{2\,m_a - 1}{1 - m_a}\,, \qquad \alpha_b = \frac{2\,m_b - 1}{1 - m_b} \tag{22}$$

The factor b verifies the equation (23) as follows

$$\int_{x_0-c}^{x_0+c} b\,(x-x_0+c)^{\alpha_a} dx + \int_{\hat{x}_s}^{x_0+c} b\,k\,(x-x_s)^{\alpha_b} dx = 1 \tag{23}$$

Therefore, the global M function is given by equations (24) and (25).
From equation (25), we obtain k which is given by equation (26).
In equation (26), $M(x)$ and x are considered for all reinjected points verifying $x_s \le x \le x_0 - c$. We calculate k as an average of equation (26) evaluated for all these values.

4. Applications. Numerical results

In this section, we present two numerical examples of the theoretical cases described in the previous section. To verify the generality of the methodology, the first one uses type V intermittency, and the second analyzes type I intermittency.
To accomplish the numerical tests, we make an iterative process using the corresponding map. Later, we divide the laminar interval L into N_s sub-intervals, and finally, we estimate the reinjection's histogram and the numerical RPD function. To do it, we utilize N reinjected points inside the laminar interval. Typically, millions of iterations are required. This procedure has been applied previously [1, 29, 31, 33, 37].

4.1 Case 1. Type V intermittency with overlapping in the lower part of the laminar interval

Let us introduce the following map [38] in equation (27) (see below), where $F(x_m) = y_m = 1$, $\hat{x}$ is the lower boundary of reinjection, and ε is the control parameter. This map has a fixed point $x = 0$ for $\varepsilon = 0$. If $0 < \varepsilon \ll 1$, type V intermittency occurs. Figure 1 shows the map for $a_1 = 0.9$, $a_2 = 2$, $\varepsilon = 0.001$, and $\hat{x} = -0.2$. To evaluate the equations described in Section 3, we analyze the following test: $a_1 = 0.9$, $a_2 = 2$, and $\varepsilon = 0.001$, $\hat{x} = -0.2$, $c = 0.114$, and $N = 100000$, where N is the number of reinjected points. We obtain $k = 0.1868$, $b = 7.25689$, $m_a = 0.4077\,(\alpha_a = -0.3117)$, $m_b = 0.4518\,(\alpha_b = -0.1757)$. Figures 2 and 3 show the complete $M(x)$ function and the RPD function, respectively. The $M(x)$ function is given by equations (16)-(17), and the RPD function is determined by Equation (12). From the figures, we observe that the theory here described works accurately regarding the numerical results. Note that the M function is non-differentiable at $x_s = -0.1016$, and the RPD function is discontinued at that point.

4.2 Case 2. Type I intermittency with overlapping in the upper part of the laminar interval

In a recent paper, the reinjection mechanism for type I intermittency in the logistic map was studied

For $x < x_s$

$$M(x) = \frac{\int_{x_0-c}^{x} y\,\phi_a(y)\,dy}{\int_{x_0-c}^{x} \phi_a(y)\,dy} = \frac{x(1+\alpha_a) + x_0 - c}{2+\alpha_a} \tag{24}$$

For $x \geq x_s$

$$\begin{aligned} M(x) &= \frac{\int_{x_0-c}^{x} y\,\phi_a(y)\,dy + \int_{x_s}^{x} y\,\phi_b(y)\,dy}{\int_{x_0-c}^{x} \phi_a(y)\,dy + \int_{x_s}^{x} \phi_b(y)\,dy} \\ &= \frac{(x-x_0+c)^{1+\alpha_a}(x_0-c+x(1+\alpha_a))\,(1+\alpha_b)(2+\alpha_b) + k\,(x-x_s)^{1+\alpha_b}(x_s+x(1+\alpha_b))\,(1+\alpha_a)(2+\alpha_a)}{(2+\alpha_b)(2+\alpha_a)\,((x-x_0+c)^{1+\alpha_a}\,(1+\alpha_b) + k\,(x-x_s)^{1+\alpha_a}\,(1+\alpha_a))} \end{aligned} \tag{25}$$

$$k = \frac{(x-x_0+c)^{1+\alpha_a}(x_0-c+x(1+\alpha_a))\,(1+\alpha_b)\,(2+\alpha_b) - M(x)\,(2+\alpha_b)\,(2+\alpha_a)\,(x-x_0+c)^{1+\alpha_a}\,(1+\alpha_b)}{M(x)\,(2+\alpha_b)\,(2+\alpha_a)\,(1+\alpha_a)\,(x-x_s)^{1+\alpha_a} - (x-x_s)^{1+\alpha_b}(x_s+x(1+\alpha_b))\,(1+\alpha_a)\,(2+\alpha_a)} \tag{26}$$

$$F(x) = \begin{cases} F_1(x) = a_1\,x + \varepsilon\,, & \hat{x} \leq x < 0 \\ F_2(x) = a_2\,x + \varepsilon\,, & 0 \leq x < x_m \\ F_3(x) = \hat{x} + (y_m - \hat{x})\left(\frac{y_m - x}{y_m - x_m}\right)^{\gamma}, & x_m \leq x \leq y_m \end{cases} \tag{27}$$

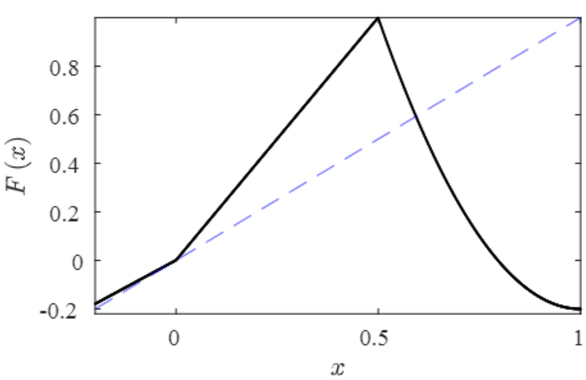

Figure 1 Map given by equation (27) for $a_1 = 0.9$, $a_2 = 2$, $\varepsilon = 0.001$, and $\hat{x} = -0.2$. Black line: map. Blue dashed line: bisector.

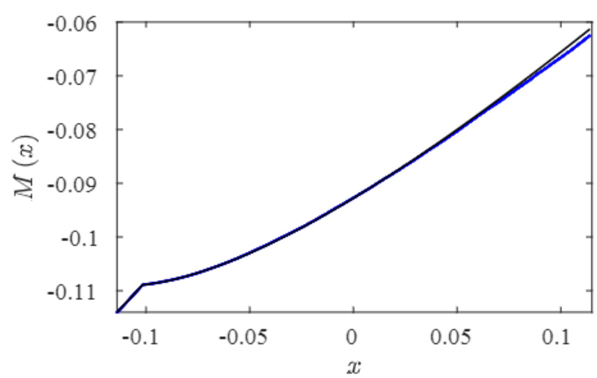

Figure 2 The complete M function given by equations (16)-(17) for $a_1 = 0.9$, $a_2 = 2$, $\varepsilon = 0.001$, and $\hat{x} = -0.2$. Blue line: numerical $M(x)$ function. Black line: theoretical $M(x)$ function.

[36]. Here, we use the results of this paper to verify the theory developed in the previous section. Because the logistic map displays type I intermittency close a period-3 window, the third iterate of this map is studied in equation (28),

$$x_{n+1} = I_\mu^3(x_n) \tag{28}$$

where the equation (29)

$$I_\mu(x) = \mu\, x\, (1-x) \tag{29}$$

is the logistic map.

We consider the fixed point $x_0 = 0.5143552770619905$. We shift the third iteration of the logistic map, $I_\mu^3(x)$, so that the fixed point x_0 matches the origin of the coordinate system. Then, the map results in equation (30),

$$\begin{aligned} F(x) = & -x_0 + \mu^3 \left(1-(x+x_0)\right)(x+x_0)\left(1+\mu\left(-1+(x+x_0)\right)(x+x_0)\right) \\ & \times\left(1+\mu^2\left(-1+(x+x_0)\right)(x+x_0)\left(1+\mu\left(-1+(x+x_0)\right)(x+x_0)\right)\right) \end{aligned} \tag{30}$$

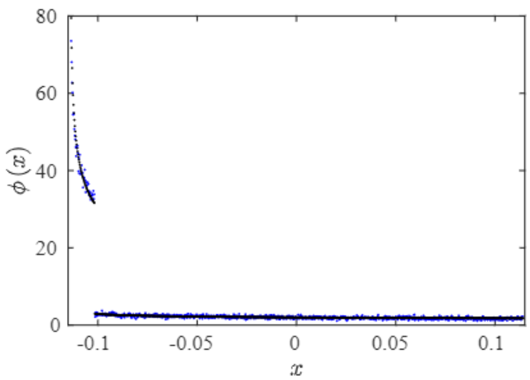

Figure 3 RPD function given by map given by equation (12) for $a_1 = 0.9$, $a_2 = 2$, $\varepsilon = 0.001$, and $\hat{x} = -0.2$. Black points: theoretical RPD function. Blue points: numerical RPD function.

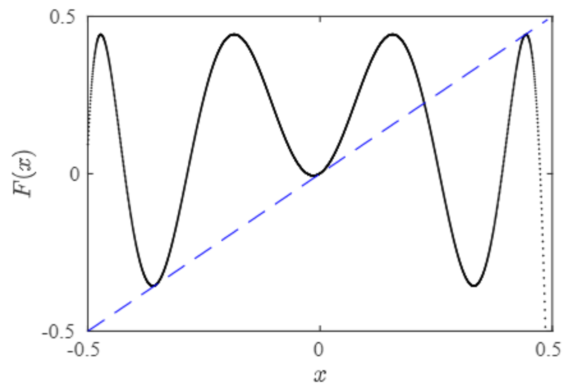

Figure 4 Map given by equation (30) for $\mu = 3.8278$. Black points: map. Blue dashed line: bisector.

For $\mu_c = 1+\sqrt{8}$, a period-3 cycle is a solution of the logistic map. However, for $\mu < \mu_c$ but near it, there is a tangent bifurcation, and type I intermittency occurs. Figure 4 shows the map given by equation (30) for $\mu = 3.8278 < \mu_c$.

For the map given by equation (30), the reinjection process around the fixed point depends on the relation between c_l, c_d and the laminar interval semi-amplitude, c ($L = [-c, c]$). The parameter c_l verifies $F(-c_l) = c_l$, and it is the laminar interval limit where there are pre-reinjection points close to $-c$. For $c \le c_l$ there is reinjection from neighboring points to points to $-c$. The parameter c_d, satisfies $\left.\frac{d\,F(x)}{d\,x}\right|_{x=c_d} = 0$ and $F(c_d) \in L$.

For the sub-interval $|c_d| \le c \le c_l$ the map shows two reinjection mechanisms, then the RPD function possesses two components. The first one is produced by pre-reinjection points away from the laminar interval, and the trajectories going by for these pre-reinjection points are reinjected in the complete laminar interval,

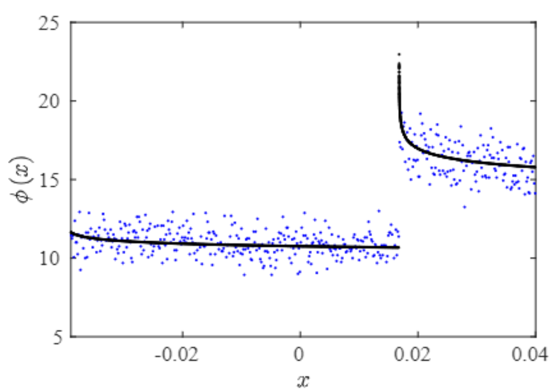

Figure 5 RPD functions for $\mu = 3.8278$ and $c = 0.04$. Black line: the RPD obtained using the theoretical development of the previous section. Blue points: the numerical RPD function. $\alpha_a = -0.0168018$, $\alpha_b = -0.0981602$.

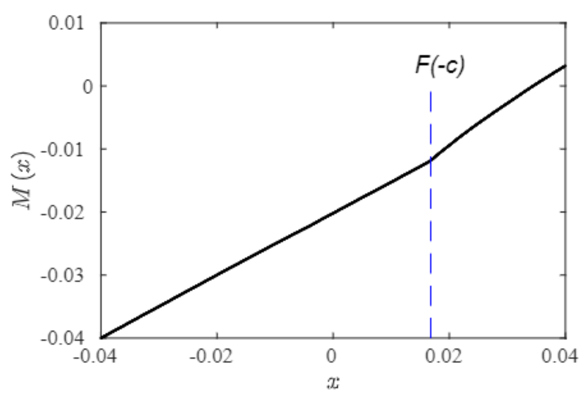

Figure 6 $M(x)$ function for $\mu = 3.8278$ and $c = 0.04$. The green line corresponds to $x_s = F(-c) = 0.0167937$.

$L = [-c, c]$. The second component is given by pre-reinjection points neighboring to the laminar interval lower limit, and they satisfy $F(x_{n-1}) \in (F(-c), c]$, where x_{n-1} are the pre-reinjection points [36].

To study the reinjection processes, we consider the following test: $\mu = 3.8278$ and $|c_d| = 0.014355277062 < c = 0.04 < c_l = 0.058036869$.

The RPD function, $\phi(x)$, is calculated by adding two reinjection mechanisms described by $\phi_a(x)$ and $\phi_b(x)$. To get the slopes m_a and m_b, we study each reinjection mechanism individually. We order the numerical data and apply the M function methodology described in Section 2.

The RPD function is shown in Figure 5. The blue points are the numerical data, and the black line is the theoretical RPD. The RPD function shows two distinct behaviors, one for $x < x_s$, and another for $x \geq x_s$. Where $x_s = F(-c)$.

For the same test, the $M(x)$ function is displayed in Figure 6. We notice the $M(x)$ function has a non-differentiable point at $x_s = F(-c)$, where the RPD function is discontinuous.

5. Conclusions

In this paper, we presented a systematic methodology to obtain the reinjection probability density function in chaotic intermittency when there are two overlapping reinjection processes. We extended the M function methodology developed and verified in previous studies [1][29–32][34].

Two different cases were studied and described. The first one considers that the overlapping occurs in the lower part of the laminar interval. The second case assumes an overlapping in the upper part of the laminar interval. For both cases, we developed theoretical equations for $M(x)$ and RPD functions.

To satisfy the normalization condition, we introduced a new real parameter called here k. This parameter takes into account the different number of reinjected points in both sub-intervals that make up the complete laminar interval.

We have verified the accurate behavior of the theoretical background here introduced by comparison with numerical data. We carried out two numerical tests. The first one studied the overlapping close to the lower part of the laminar interval, and the second test analyzed the reinjection mechanism when there is overlapping in the upper part of the laminar interval. One test considered type V intermittency, and another one used type I intermittency. In both tests, the theoretical results are very accurate regarding the numerical data.

6. Declaration of competing interest

We declare that we have no significant competing interests, including financial or non-financial, professional, or personal interests interfering with the full and objective presentation of the work described in this manuscript.

7. Acknowledgements

The authors are grateful to Universidad Nacional de Córdoba and Universidad Politécnica de Madrid.

8. Funding

This work was supported by SECyT of Universidad Nacional de Córdoba, and Ministerio de Ciencia, Innovación y Universidades of Spain under grand No RTI2018-094409-B-I00.

9. Author contributions

S.E. Conceptualization, methodology, software, validation, formal analysis, investigation, resources, writing the paper, visualization, supervision, project administration, and funding acquisition. E.dR. Methodology, validation, formal analysis, resources, writing the paper, supervision, and funding acquisition. M.G. Numerical results and Validation. All authors have read and agreed to the published version of the manuscript.

10. Data availability statement

The authors confirm that the data supporting the findings of this study are available within the article [and/or] its supplementary materials.

References

[1] S. Elaskar and E. Del Río, *New advances on chaotic intermittency and its applications.* Springer, 2017.

[2] H. G. Schuster and W. Just, *Deterministic chaos.* John Wiley & Sons, 2005.

[3] A. H. Nayfeh and B. Balachandran, *Applied nonlinear dynamics.* John Wiley & Sons, 1995.

[4] G. Pizza, C. E. Frouzakis, and J. Mantzaras, "Chaotic dynamics in premixed hydrogen/air channel flow combustion," *Combustion Theory and Modelling*, vol. 16, no. 2, pp. 275–299, 2012.

[5] P. De Anna, T. Le Borgne, M. Dentz, A. M. Tartakovsky, D. Bolster, and P. Davy, "Flow intermittency, dispersion, and correlated continuous time random walks in porous media," *Physical review letters*, vol. 110, no. 18, p. 184502, 2013.

[6] C. Stan, C. Cristescu, and D. Dimitriu, "Analysis of the intermittent behavior in a low-temperature discharge plasma by recurrence plot quantification," *Physics of Plasmas*, vol. 17, no. 4, p. 042115, 2010.

[7] A. Chian, *Complex systems approach to economic dynamics.* Springer Science & Business Media, 2007.

[8] J. Żebrowski and R. Baranowski, "Type i intermittency in nonstationary systems—models and human heart rate variability," *Physica A: Statistical Mechanics and Its Applications*, vol. 336, no. 1-2, pp. 74–83, 2004.

[9] P. Paradisi, P. Allegrini, A. Gemignani, M. Laurino, D. Menicucci, and A. Piarulli, "Scaling and intermittency of brain events as a manifestation of consciousness," in *AIP Conference Proceedings*, vol. 1510, no. 1. American Institute of Physics, 2013, pp. 151–161.

[10] J. Bragard, J. Vélez, J. Riquelme, L. Pérez, R. Hernández-García, R. Barrientos, and D. Laroze, "Study of type-iii intermittency in the landau–lifshitz-gilbert equation," *Physica Scripta*, vol. 96, no. 12, p. 124045, 2021.

[11] P. Ge and H. Cao, "Intermittent evolution routes to the periodic or the chaotic orbits in rulkov map," *Chaos: An Interdisciplinary Journal of Nonlinear Science*, vol. 31, no. 9, p. 093119, 2021.

[12] I. Belyaev, D. Biryukov, D. N. Gerasimov, and E. Yurin, "On-off intermittency and hard turbulence in the flow of fluid in the magnetic field," *Chaos: An Interdisciplinary Journal of Nonlinear Science*, vol. 29, no. 8, p. 083119, 2019.

[13] P. Bordbar and S. Ahadpour, "Type-i intermittency from markov binary block visibility graph perspective," *Journal of Applied Statistics*, vol. 48, no. 7, pp. 1303–1318, 2021.

[14] L.-W. Kong, H. Fan, C. Grebogi, and Y.-C. Lai, "Emergence of transient chaos and intermittency in machine learning," *Journal of Physics: Complexity*, vol. 2, no. 3, p. 035014, 2021.

[15] S. G. Stavrinides, A. N. Miliou, T. Laopoulos, and A. Anagnostopoulos, "The intermittency route to chaos of an electronic digital oscillator," *International Journal of Bifurcation and Chaos*, vol. 18, no. 05, pp. 1561–1566, 2008.

[16] S. Zambrano, I. P. Mariño, and M. A. Sanjuán, "Controlling crisis-induced intermittency using its relation with a boundary crisis," *New Journal of Physics*, vol. 11, no. 2, p. 023025, 2009.

[17] P. Manneville and Y. Pomeau, "Intermittency and the lorenz model," *Physics Letters A*, vol. 75, no. 1-2, pp. 1–2, 1979.

[18] M. Bauer, S. Habip, D.-R. He, and W. Martienssen, "New type of intermittency in discontinuous maps," *Physical review letters*, vol. 68, no. 11, p. 1625, 1992.

[19] D.-R. He, M. Bauer, S. Habip, U. Krueger, W. Martienssen, B. Christiansen, and B.-H. Wang, "Type v intermittency," *Physics Letters A*, vol. 171, no. 1-2, pp. 61–65, 1992.

[20] J. Fan, F. Ji, S. Guan, B.-H. Wang, and D.-R. He, "The distribution of laminar lengths in type v intermittency," *Physics Letters A*, vol. 182, no. 2-3, pp. 232–237, 1993.

[21] T. Price and T. Mullin, "An experimental observation of a new type of intermittency," *Physica D: Nonlinear Phenomena*, vol. 48, no. 1, pp. 29–52, 1991.

[22] N. Platt, E. Spiegel, and C. Tresser, "On-off intermittency: A mechanism for bursting," *Physical Review Letters*, vol. 70, no. 3, p. 279, 1993.

[23] J. Heagy, N. Platt, and S. Hammel, "Characterization of on-off intermittency," *Physical Review E*, vol. 49, no. 2, p. 1140, 1994.

[24] A. Pikovsky, G. Osipov, M. Rosenblum, M. Zaks, and J. Kurths, "Attractor-repeller collision and eyelet intermittency at the transition to phase synchronization," *Physical review letters*, vol. 79, no. 1, p. 47, 1997.

[25] A. Pikovsky, M. Rosenblum, and J. Kurths, "Synchronization: a universal concept in nonlinear science," 2002.

[26] M. Kurovskaya, "Distribution of laminar phases at eyelet-type intermittency," *Technical Physics Letters*, vol. 34, no. 12, pp. 1063–1065, 2008.

[27] A. E. Hramov, A. A. Koronovskii, M. K. Kurovskaya, and S. Boccaletti, "Ring intermittency in coupled chaotic oscillators at the boundary of phase synchronization," *Physical review letters*, vol. 97, no. 11, p. 114101, 2006.

[28] J. Hirsch, B. Huberman, and D. Scalapino, "Theory of intermittency," *Physical Review A*, vol. 25, no. 1, p. 519, 1982.

[29] S. Elaskar, E. Del Rio, and J. M. Donoso, "Reinjection probability density in type-iii intermittency," *Physica A: Statistical Mechanics and its Applications*, vol. 390, no. 15, pp. 2759–2768, 2011.

[30] E. del Rio, S. Elaskar, and V. A. Makarov, "Theory of intermittency applied to classical pathological cases," *Chaos: An Interdisciplinary Journal of Nonlinear Science*, vol. 23, no. 3, p. 033112, 2013.

[31] E. del Rio, S. Elaskar, and J. M. Donoso, "Laminar length and characteristic relation in type-i intermittency," *Communications in Nonlinear Science and Numerical Simulation*, vol. 19, no. 4, pp. 967–976, 2014.

[32] G. Krause, S. Elaskar, and E. del Río, "Noise effect on statistical properties of type-i intermittency," *Physica A: Statistical Mechanics and its Applications*, vol. 402, pp. 318–329, 2014.

[33] S. Elaskar, E. del Rio, G. Krause, and A. Costa, "Effect of the lower boundary of reinjection and noise in type-ii intermittency," *Nonlinear Dynamics*, vol. 79, no. 2, pp. 1411–1424, 2015.

[34] S. Elaskar and E. Del Río, "Discontinuous reinjection probability density functions in type v intermittency," *Journal of Computational and Nonlinear Dynamics*, vol. 13, no. 12, p. 121001, 2018.

[35] S. Elaskar, E. Del Rio, and A. Costa, "Reinjection probability density for type-iii intermittency with noise and lower boundary of reinjection," *Journal of Computational and Nonlinear Dynamics*, vol. 12, no. 3, p. 031020, 2017.

[36] S. Elaskar, E. del Río, and S. Elaskar, "Intermittency reinjection in the logistic map," *Symmetry*, vol. 14, no. 3, p. 481, 2022.

[37] S. Elaskar, E. del Río, and W. Schulz, "Analysis of the type v intermittency using the perron-frobenius operator,"

Symmetry, vol. 14, p. 2519, 2022.

[38] S. Elaskar, E. del Río, and L. Gutierrez Marcantoni, "Nonuniform reinjection probability density function in type v intermittency," *Nonlinear Dynamics*, vol. 92, p. 683697, 2018.